Acta metall. mater. Vol. 40, No. 1, pp. 43–55, 1992
Printed in Great Britain. All rights reserved

0956-7151/92 $5.00 + 0.00
Copyright © 1991 Pergamon Press plc

MICROSTRUCTURAL SIMULATION OF DYNAMIC RECRYSTALLIZATION

A. D. ROLLETT[1], M. J. LUTON[2] and D. J. SROLOVITZ[3]

[1]Mail Stop K765, Los Alamos National Laboratory, Los Alamos, NM 87545, [2]Corporate Research, Exxon Research and Engineering Company, Annandale, NJ 08801 and [3]Department of Materials Science and Engineering, University of Michigan, Ann Arbor, MI 48109, U.S.A.

(Received 10 January 1991; in revised form 12 June 1991)

Abstract—A Monte Carlo model for dynamic recrystallization has been developed from earlier models used to simulate static recrystallization and grain growth. The model simulates dynamic recrystallization by adding recrystallization nuclei and stored energy continuously with time. The simulations reproduce many of the essential features of dynamic recrystallization. The stored energy of the system, which may be interpreted as a measure of the flow stress, goes through a maximum and then decays, monotonically under some conditions and in an oscillatory manner under others. The principle parameters that were studied were the rate of adding stored energy, ΔH, and the rate of adding nuclei, ΔN. As ΔH increases, for fixed ΔN, the oscillations decay more rapidly and the asymptotic energy rises. As ΔN increases, again the oscillations decay more rapidly but the asymptotic stored energy decreases. The mean grain size of the system also oscillates in a similar manner to the stored energy but out of phase by 90°. The flow stress oscillations occurred for conditions which lead to both coarsening and refinement of the initial grain size. Necklacing of the prior grain structure by new grains were observed for low ΔH and high ΔN; it is, however, not an invariable feature of grain refinement. The initial grain size has a profound influence on the microstructure that evolves during the first cycle of recrystallization but at long times, a mean grain size is established which depends on the values of ΔH and ΔN alone. Comparison of the relationships between the energy storage rate, maximum and asymptotic stored energy and the grain size suggest that in physical systems the energy storage rate and the nucleation rate are coupled. Comparison of the simulation results with experimental trends suggests that the dependence of nucleation rate on storage should be positive but weak. All of these results were obtained without the addition of special parameters to the model.

Résumé—On développe un modèle de MONTE CARLO pour la recristallisation dynamique à partir de modèles antérieurs utilisés pour simuler la recristallisation statique et la croissance des grains. Le modèle simule la recristallisation dynamique en ajoutant des germes de recristallisation et une énergie emmagasinée en continu avec le temps. Les simulations reproduisent plusieurs aspects essentiels de la recristallisation dynamique. L'énergie emmagasinée du système, qui peut être interprêtée comme une mesure de la contrainte d'écoulement, passe par un maximum, puis décroît d'une manière monotone dans certaines conditions et avec des oscillations dans d'autres conditions. Les paramètres principaux qui sont étudiés sont la vitesse d'accumulation de l'énergie stockée ΔH et la vitesse d'addition de germes ΔN. Lorsque ΔH s'élève, pour ΔN fixe, les oscillations décroissent plus rapidement et l'énergie asymptotique s'élive. Lorsque ΔN croît, les oscillations décroissent encore plus rapidement, mais l'énergie emmagasinée asymptotique diminue. La taille moyenne de grains du système oscille aussi de la même manière que l'énergie emmagasinée, mais avec un déphasage de 90°. Les oscillations de la contrainte d'écoulement se produisent dans des conditions qui conduisent tant au grossissement qu'à l'affinage de la taille initiale de grains. Pour de faibles ΔN et des ΔN élevés, on observe la formation d'un collier de nouveaux grains dans la structure initiale; cependant ce n'est pas un aspect invariable de l'affinage des grains. La taille initiale des grains a une influence profonde sur la microstruture qui évolue pendant le premier cycle de recristallisation mais, pour des longs, on établit une taille moyenne des grains qui dépend seulement des valeurs de ΔH et de ΔN. La comparaison des relations entre la vitesse de stockage de l'énergie, l'énergie, emmagasinée maximale et asymptotique et la taille des grains suggère que, dans les systèmes physiques, la vitesse de stockage de l'énergie et la vitesse de germination sont couplées. La comparaison des résultats des simulations avec les courbes expérimentales suggère que la dépendance de la vitesse de germination vis à vis du stockage doit être positive, mais faible. Tous ces résultats sont obtenus sans ajouter de paramètres spéciaux au modèle.

Zusammenfassung—Es wird ein Monte-Carlo-Modell der dynamischen Rekristallisation aus früheren Modellen, die für die Simulation statischer Rekristallisation und des Kornwachstums benutzt wurden, entwickelt. Das Modell simuliert die dynamische Rekristallisation, indem Rekristallisationskeime und gespeicherte Energie kontinuierlich mit der Zeit zugefügt werden. Die simulationen ergeben viele wesentliche Erscheinungen der dynamischen Rekristallisation. Die gespeicherte Energie des Systems, die als ein Maß für die Fließspannung angesehen werden kann, geht durch ein Maximum und fällt dann monoton oder oszillatorisch je nach Bedingungen ab. Die untersuchten Hauptparameter sind die Rate ΔH, mit der gespeicherte Energie zugeführt wird, und die Rate ΔN, mit der Keime zugefügt werden. Nimmt

ΔH bei festem ΔN zu, dann klingen die Oszillationen schneller ab und die asymptotische Energie nimmt zu. Nimmt ΔN zu, dann fallen die Oszillationen wiederum rascher ab, aber die asymptotische gespeicherte Energie nimmt ab. Die mittlere Korngröße des Systems oszilliert ähnlich wie die gespeicherte Energie, jedoch um 90° außer Phase. Die Fließspannungsoszillationen treten bei Bedingungen auf, die sowohl zu Vergröberung als auch zu Verfeinerung der anfänglichen Korngröße führen. Die Dekoration der alten Kornstruktur durch neue Körner findet sich bei niedrigem ΔH und hohem ΔN; allerdings ist das keine beständige Eigenschaft der Kornverfeinerung. Die anfängliche Korngröße beeinflußt die Mikrostruktur stark, die sich während des ersten Zyklus der Rekristallisation einstellt; bei langen Zeiten ergibt sich allerdings eine mittlere Korngröße, die von ΔH und ΔN alleine abhängt. Vergleich der Beziehungen zwischen Energiespeicherungsrate, maximaler und asymptotischer gespeicherter Energie und der Korngöße legt die Vorstellung nahe, daß in physikalischen Systemen Energiespeicherungsrate und Keimbildungsrate gekoppelt sind. Der Vergleich der Simulationsergebnisse mit den experimentell bestimmten Zusammenhängen legt nahe, daß die Abhängigkeit der Keimbildungsrate von der Speicherung positiv, aber schwach sein sollte. Sämtliche Ergebnisse werden ohne Einführung spezieller Parameter im Modell erhalten.

1. INTRODUCTION

When crystalline materials are plastically deformed at homologous temperatures in excess of 0.5 two characteristic types of behavior are observed, which appear to depend on the stacking fault energy of the material. In high stacking fault energy materials, the generation and accumulation of dislocations due to the plastic strain is continuously offset by dislocation rearrangement and annihilation by dynamic recovery. At high strains, the latter process balances dislocation generation and further strain is accommodated at a constant flow stress. In medium-to-low stacking fault energy materials dynamic recovery is less rapid, however, and relatively dislocation-free regions can form and grow into the dislocated surrounding material. These recrystallized regions are separated from the adjacent dislocated material by high angle grain boundaries which act as sinks for matrix dislocations. This process is known as dynamic recrystallization. The term "dynamic" is used to signify recrystallization that occurs continually during plastic deformation.

The earliest observations of dynamic recrystallization in metals were made during the study of creep in lead and lead alloys [1–3]. Here it was found that periods of accelerated creep were associated with the formation of newly recrystallized grains [2, 3]. At about the same time, Steinemann [4] showed that thin films of ice would recrystallize when subjected to stress, a process he called "kinematic recrystallization". In the late 1960s research on dynamic recrystallization focused on the occurrence of this phenomenon during the hot working of metals [5–11], since it was perceived that it could play an important role in determining the type of microstructures developed during extrusion, forging and hot strip rolling. Initially there was considerable debate as to whether the phenomenon occurred at all during deformation at the high rates typical of working operations. Such arguments were largely due to the lack of unequivocal evidence for the appearance of new grains during deformation, which arose because of the difficulty of ensuring rapid quenching of the deformed structures. Ultimately, sufficient evidence was obtained to unambiguously establish the occurrence of dynamic recrystallization in f.c.c. metals of medium to low stacking fault energy.

The occurrence of dynamic recrystallization, under constant strain rate conditions, is often accompanied by flow stress oscillations [5–7]. As shown in Fig. 1, at low strain rates or high temperatures, the flow curves are characterized by flow stress oscillations at low strains which gradually become damped to give an apparent steady state flow at high strains. By contrast, at high strain rates or low temperatures, a single broad initial peak is observed which is followed by a gradual decrease in flow stress with strain, to a steady state value. This steady state flow stress is not what is meant classically by the term flow stress because the material state is far from homogeneous on a microscopic scale. Instead, the flow stress is an average over the deforming volume of material.

Early attempts at modelling dynamic recrystallization focused on explaining the initial peak in flow stress and the transition from periodic to single peak behavior. Luton and Sellars [7] analyzed the dynamic recrystallization process in terms of the incubation strain for the onset of recrystallization, ϵ_c, and the

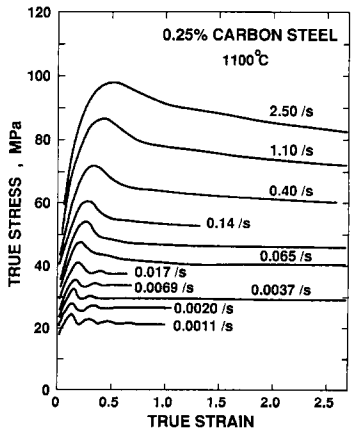

Fig. 1. Classical series of oscillatory flow curves for 0.25%-carbon steel obtained at 1100°C and strain rates between 1.1×10^{-3} and $2.5\ s^{-1}$. After Rossard and Blain [6].

strain or time required for completion of the recrystallization process, ϵ_x. They argued that these two quantities exhibit different stress dependencies and when $\epsilon_c > \epsilon_x$, one complete recrystallization cycle is finished before the next begins and an oscillatory flow curve is predicted. On the other hand, when $\epsilon_c < \epsilon_x$, a second wave of recrystallization starts before the first recrystallization cycle is completed and hence the oscillatory behavior of the flow curve is suppressed. The strain to the initial peak in flow stress, ϵ_p, has generally been taken as a measure of ϵ_c and this has provided a simple means of determining the stress and temperature dependence of this quantity. It has been shown experimentally, however, that newly recrystallized grains are first observed at $\sim 0.8\,\epsilon_p$ [8]. Sah *et al.* [9] refined the original model to account for the influence of grain size changes on the recrystallization kinetics and thereby explained the gradual damping of the flow stress oscillations at high strains. More formal treatment followed [10, 11] which provided a dislocation-mechanics basis for the observations. The model of Sandström and Lagneborg [11] is based on the evolution of the distribution of dislocation density within the material and effectively accounts for the transition from periodic to single peak behavior and the gradual disappearance of flow stress oscillations with strain. Recently, detailed metallographic studies by Sakai and co-workers [12–14] have shown that the transition from single to multipeak behavior depends on the relationship between the initial grain size, R_0, and that established under steady state flow conditions, R_∞. It was shown that flow stress oscillations occur when $R_0 < 2R_\infty$. These observations have been interpreted in terms of a nucleus selection model by Sakai and Jonas [4, 15]. Although this criterion appears to work well for carbon steels [12, 13], it does not provide a good description of some observations in copper and copper alloys [16, 17] and microalloyed steels [18, 19]. It is evident that, during dynamic recrystallization, the interaction between work-hardening and repeated cycles of recrystallization lead to a rather complex evolution of microstructure. Accordingly, a complete understanding of the phenomenon requires these effects to be properly taken into account.

The objective of the work described in this paper is to develop a simple model for dynamic recrystallization by extension of the procedures used to account for the microstructural evolution during grain growth and static recrystallization [20–23]. The recrystallization model is a two-dimensional Monte Carlo simulation method which uses stored energy to represent the dislocation content of the materials. The details of the simulation procedure are described in the following section. The dynamic recrystallization simulation method is then employed to study the effects of strain rate, nucleation rate and initial grain size on the flow curves, and the evolution of grain size.

2. SIMULATION PROCEDURE

The computer model employed in this work is based upon the same Monte Carlo model developed previously for the simulation of grain growth [20, 21] and static recrystallization [22, 23]. The microstructure is mapped onto a two-dimensional triangular lattice by assigning each lattice site an index S_i which represents the crystallographic orientation of the material in the vicinity of the site. A contiguous group of sites that all have the same index are part of the same grain, while nearest neighbor sites with unlike indices are separated by a grain boundary. To account for work-hardening within the grains, stored energy, proportional to the local dislocation density, is assigned to each site. Hence, for the case of isotropic grain boundary energy, the total energy of the system is

$$E = \frac{J}{2}\sum_{i}^{n}\sum_{j}^{m}(1 - \delta_{S_i S_j}) + \sum_{i}^{n} H_{S_i} \qquad (1)$$

where J scales the grain boundary energy, the first sum is over all of the sites in the model ($n = 40{,}000$), the second sum is over the nearest neighbors of site i ($m = 6$), and δ_{ab} is the Kronecker delta function. H_S is the stored energy associated with each site of orientation S. The growth component of recrystallization is handled by employing a zero temperature Monte Carlo method which corresponds to choosing a lattice site at random, reorienting that site to a randomly chosen, different value of S and calculating the change in energy ΔE. If $\Delta E \leqslant 0$, the new orientation is retained, while if $\Delta E > 0$, the old orientation of the site is returned. The continuous time method [24] is employed to increase the efficiency of the Monte Carlo method. The unit of time in the present simulations is a Monte Carlo Step (mcs) which corresponds to n reorientation attempts. The nucleation of recrystallized grains is achieved by adding new grains to the microstructure at randomly chosen positions. These embryonic grains or nuclei are added periodically in time. Each embryo consists of three sites arranged in a triangle. Each embryo is assigned a unique orientation number S and initially assigned a stored energy of zero, that is $H = 0$. To this point, the method is identical to that employed for static recrystallization [22, 23].

To model dynamic recrystallization, however, it is necessary to allow for continuous work hardening of the material. Accordingly, the stored energy associated with every orientation number is incremented by a fixed amount, ΔH, at regular intervals during the simulation. The stored energy due to work hardening, H, is taken to be proportional to the dislocation density, ρ, which is, in turn, related to the flow stress, σ, through the relation

$$\sigma = M\alpha\mu b\sqrt{\rho} \qquad (2)$$

where M is a Taylor factor, α is a geometrical constant of order 0.5, μ is the shear modulus, and b

is the Burgers vector. Thus the linear increase of stored energy with time represents a parabolic stress–strain relation for the constant strain rate case. Other work-hardening relationships can be easily incorporated into the model and their effect will be explored in further work on this topic. By associating a particular stored energy with each orientation number, it is possible, for example, to incorporate a work-hardening relation where the hardening rate depends on the current local flow stress, which is closer to the current view of constitutive relations. It should be noted that the quoted nucleation rates are actually the rate at which potential nuclei are introduced into the system. Since the nuclei are delineated by grain boundaries, there is a grain boundary interfacial tension which tends to make these nuclei shrink away. Consequently, at low stored energies ($H/J \leqslant 2$), the rate of survival of the potential nuclei depends on the availability of prior boundaries, so that heterogeneous nucleation is dominant [23]. Hence the actual nucleation rate is less than or equal to the quoted nucleation rate (ΔN). It is important to note that the present model makes no assumption about a critical strain being required to start or complete the nucleation process. In addition, no relation between the nucleation rate and the state of work-hardening is assumed. Instead, the work-hardening rate and the nucleation rate are fixed at the beginning of each simulation run. This is unlikely to be the case in real materials, but it provides us with the opportunity of independently exploring the influence of these two quantities. Finally, the model does not include the plastic strain induced change in grain aspect ratio. This is not considered important during dynamic recrystallization, since it is well documented that the grain shape tends to remain equiaxed [25].

Simulations were performed at a fixed nucleation rate of $\Delta N = 0.2$/mcs, corresponding to 1 nucleus added every 5 mcs, and for stored energy increment rates of $\Delta H = 10^{-4}$, 2×10^{-4}, 5×10^{-4}, 10^{-3}, 2×10^{-3}, 5×10^{-3} and 10^{-2} J/mcs. Additional simulations were performed at $\Delta H = 10^{-3}$ J/mcs and for nucleation rates of $\Delta N = 0.1$, 0.2, 0.5, 1, 2 and 5 J/mcs. The starting microstructures were obtained from normal grain growth simulations. Grain sizes are always quoted in units of lattice parameters for the triangular lattice employed in the present simulations. Dynamic recrystallization studies were also performed for initial grain sizes, R_0, of 12.6, 8.9 and 6.3 with $\Delta H = 10^{-3}$ J/mcs and $\Delta N = 1$/mcs. Note that the grain size was calculated as $R = \sqrt{A}$, where A is the number of lattice sites associated with a particular grain. The data presented in the following section were obtained by averaging over five simulations under identical sets of initial and simulation conditions.

3. RESULTS

3.1. Evolution of stored energy

As stated above, the type of flow curve observed during high temperature, constant strain rate experiments provides insight into the underlying microstructural processes. Accordingly, the specific stored energy was recorded continuously during each simulation run. The stored energy is plotted as a function of time in Fig. 2(a) for a microstructure with initial grain size $R_0 = 6.3$, a fixed nucleation rate of 0.2 nuclei per mcs and energy storage rates in the range of $10^{-4} \leqslant \Delta H \leqslant 10^{-2}$ J/mcs. The stored energy rises with increasing time to a peak value and then oscillates with decreasing amplitude until an essentially constant value is obtained at long times. It is notable that oscillations in the stored energy occur at all values of the storage rate but the rate at which they decay to a constant, asymptotic value occurs more quickly with increasing storage rate. Also, the asymptotic value of the stored energy increases with increasing storage rate. Since it is likely that the rate at which potential nuclei are added to the system has a pronounced effect on the flow curves and the microstructures that are developed, simulations were also

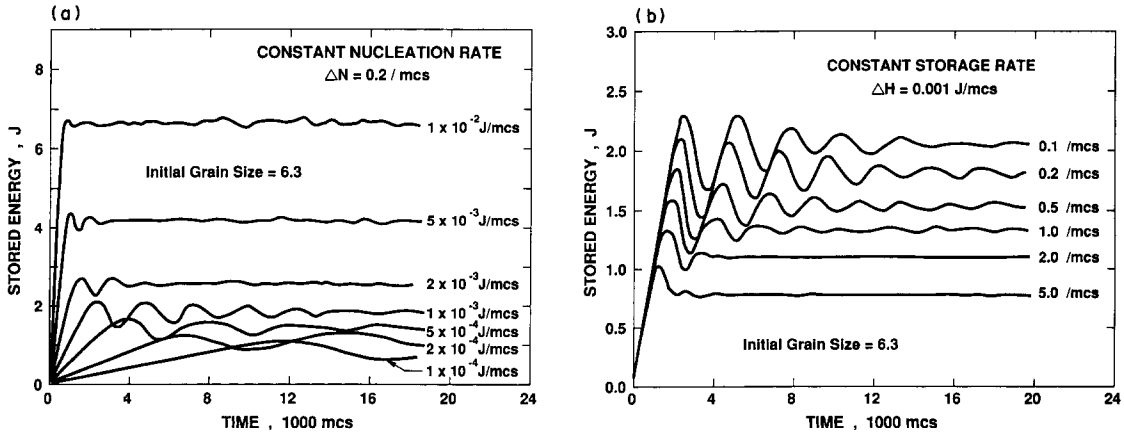

Fig. 2. (a) Plot of stored energy for a constant nucleation rate of $\Delta N = 0.2$/mcs and a range of energy addition rates, ΔH, as indicated in the figure. (b) Plot of stored energy for a constant energy addition rate of $\Delta H = 10^{-3}$ J/mcs and a range of nucleation rates, ΔN, as indicated in the figure.

performed at a fixed energy addition rate and different nucleation rates. The resulting stored energy vs time curves are shown in Fig. 2(b) for ΔN in the range of 0.1 to 5, for an initial grain size of 6.4, and for an energy storage rate of 10^{-3} per mcs. As with the case of the constant nucleation rate curves [Fig. 2(a)], the stored energy rises with increasing time, peaks at a high value and saturates at a lower, constant value at long times. Initially all the curves rise at the same rate until the stored energy reaches about 80% of the peak value. The level of the stored energy at the first peak and the asymptotic stored energy increase as the nucleation rate is decreased. It is notable that oscillations in the stored energy vs time plots occur at all values of the nucleation rate. The oscillations decay to the constant, asymptotic value of the stored energy more quickly with increasing nucleation rate. Also, the period and the amplitude of the oscillations decrease with increasing nucleation rate.

For the entire set of data represented in Fig. 2, the first maximum in the stored energy vs time plots always represents the absolute maximum stored energy in the system at any time during the dynamic recrystallization simulation. As indicated above, the peak height increased with increasing storage rate and decreasing nucleation rate. These observations are quantified in Fig. 3(a) and (b), where the maximum and asymptotic stored energy are plotted as a function of storage rate and nucleation rate, respectively. The dependence of the stored energy on the storage rate is sub-linear over the entire range of storage rates simulated, however, both the maximum asymptotic values do appear to approach a linear dependence on storage rate at large storage rates. It is apparent from these data that the ratio of the maximum to the asymptotic stored energy decreases as the storage rate increases. Figure 3(b) shows the maximum and asymptotic stored energies as a function of nucleation rate. The fitted curves are logarithmic decay curves with similar exponents so that, if plotted semi-logarithmically, the two curves would be sensibly parallel. This suggests a strong correlation between the asymptotic stored energy and

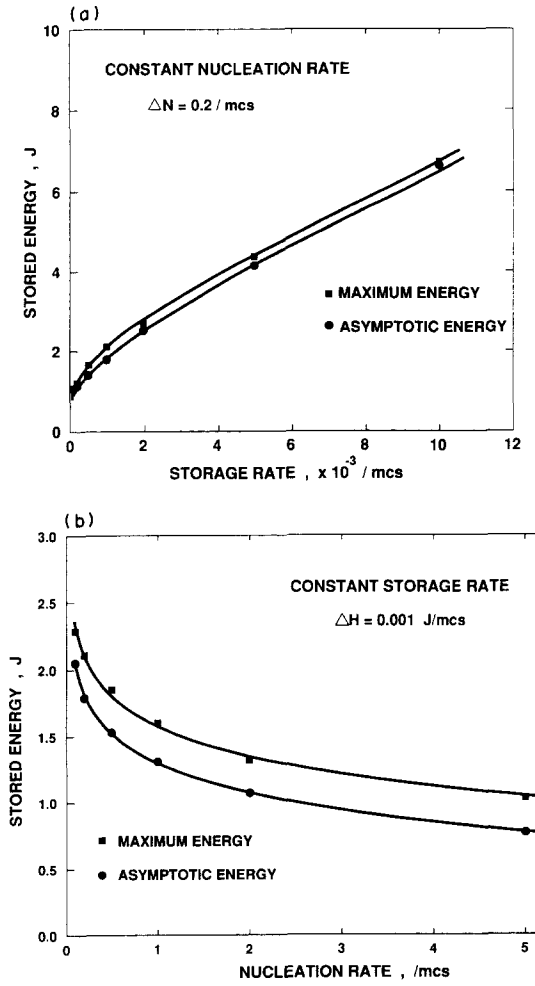

Fig. 3. Plot of the maximum and asymptotic stored energy vs (a) energy storage rate for a fixed nucleation rate of $\Delta N = 0.2$/mcs and (b) nucleation rate for a fixed energy storage rate of $\Delta H = 10^{-3}$ J/mcs.

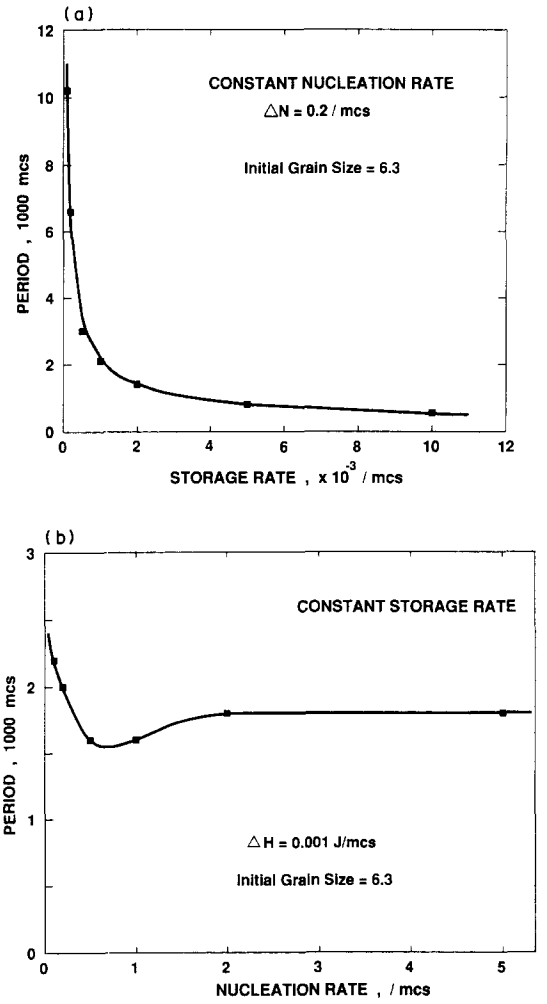

Fig. 4. Plot of the period of the stored energy oscillations vs (a) energy storage rate for a fixed nucleation rate of $\Delta N = 0.2$/mcs and (b) nucleation rate for a fixed energy storage rate of 10^{-3} J/mcs.

the maximum stored energy. The ratio of the maximum stored energy to the asymptotic stored energy varies over a small range from a low of 1.02, at the largest stored energy rate, to a high of 1.35, at the highest nucleation rate.

The curves shown in Fig. 2 indicate that the stored energy shows oscillations for all of the energy storage rates considered. For very small energy storage rates or large nucleation rates, these oscillations are strongly damped with very few oscillations visible. The period of the oscillations were estimated as twice the time span between the first peak and subsequent minimum in the stored energy. The dependence of the oscillation period on energy storage rate and nucleation rate are indicated in Fig. 4(a) and (b), respectively. The oscillation period decays rapidly with increasing energy storage rates. At fixed energy storage rate, the oscillation period decays with increasing nucleation rate for small nucleation rates but then increases at larger values of the nucleation rate. The observed minimum in the oscillation period with nucleation rate occurs for $0.5 \leqslant \Delta N \leqslant 1$ mcs.

3.2. Evolution of microstructure

The microstructural evolution during dynamic recrystallization is illustrated in Figs 5–7. Figure 5 shows the change in microstructure for a nucleation rate of 0.2 per mcs and an energy storage rate of 10^{-3} J/mcs. At short times, it is apparent that most nucleation occurred heterogeneously at prior grain boundaries. The first microstructure is taken before the first peak, at $t = 2000$ mcs, and the second just after, at $t = 3000$ mcs, showing that the peak in stored energy is not reached until a significant amount of recrystallization has taken place. The third microstructure is taken close to the maximum grain size, at $t = 4000$ mcs, and shows an obviously coarser structure than the fourth, a representative long time microstructure, taken at $t = 20{,}000$ mcs. At long times, it is apparent that some grains successfully nucleate homogeneously within prior grains. A contrasting case is shown in Fig. 6, where the energy addition rate is the same, i.e. 10^{-3} J/mcs, but the nucleation rate is 5 per mcs so that the asymptotic grain size is smaller than the initial grain size. Again, the first microstructure, taken at $t = 1000$ mcs (just before the peak in stored energy), shows that the first cycle of recrystallization is far from complete. At 2000 mcs, just before the peak in stored energy, the first cycle of recrystallization is nearly complete and the few original grains that remain have highly non-compact shapes. The microstructures at 3000 mcs and at 20,000 mcs are similar which is reasonable in view of the lack of variation in grain size or stored energy after 3000 mcs. There is some spatial variation in grain size which is expected from

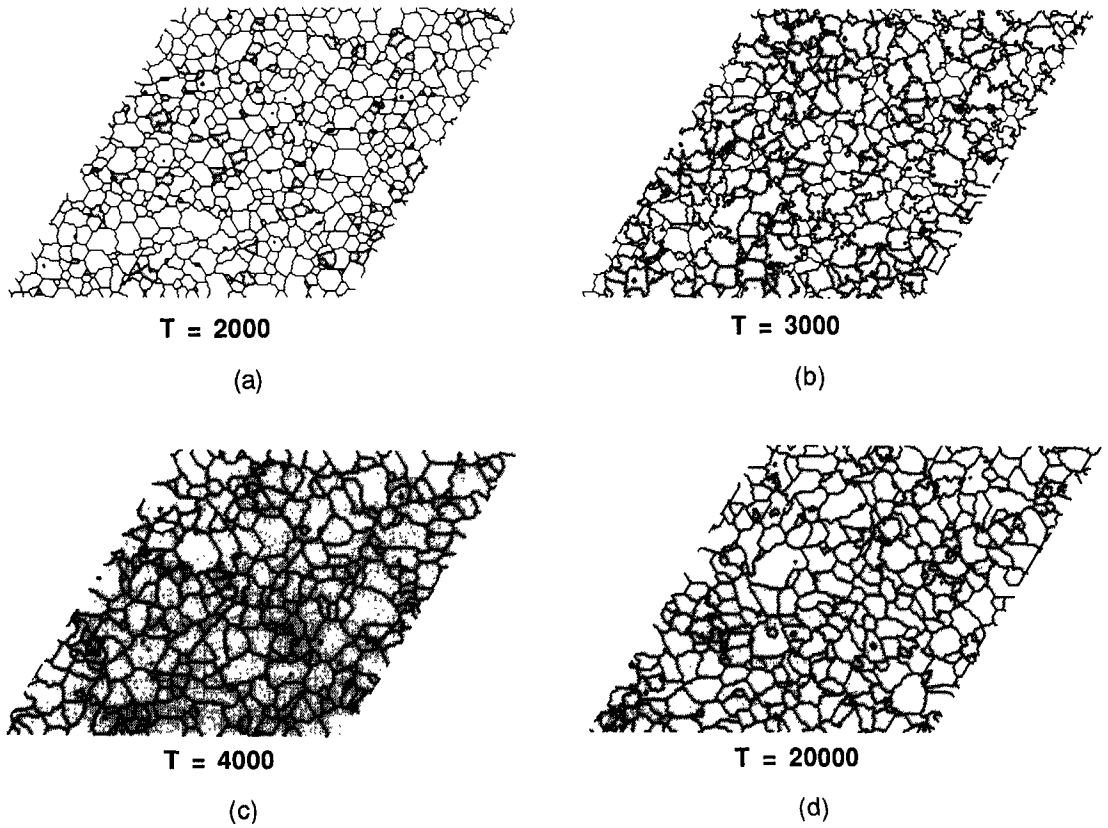

Fig. 5. Simulated microstructure generated with a nucleation rate of 0.2/mcs and an energy storage rate of 10^{-3} J/mcs at times (a) 2000 mcs (before the first stored energy peak), (b) 3000 mcs (after the first stored energy peak), (c) 4000 mcs (close to the maximum grain size) and (d) 20,000 mcs (the asymptotic grain size).

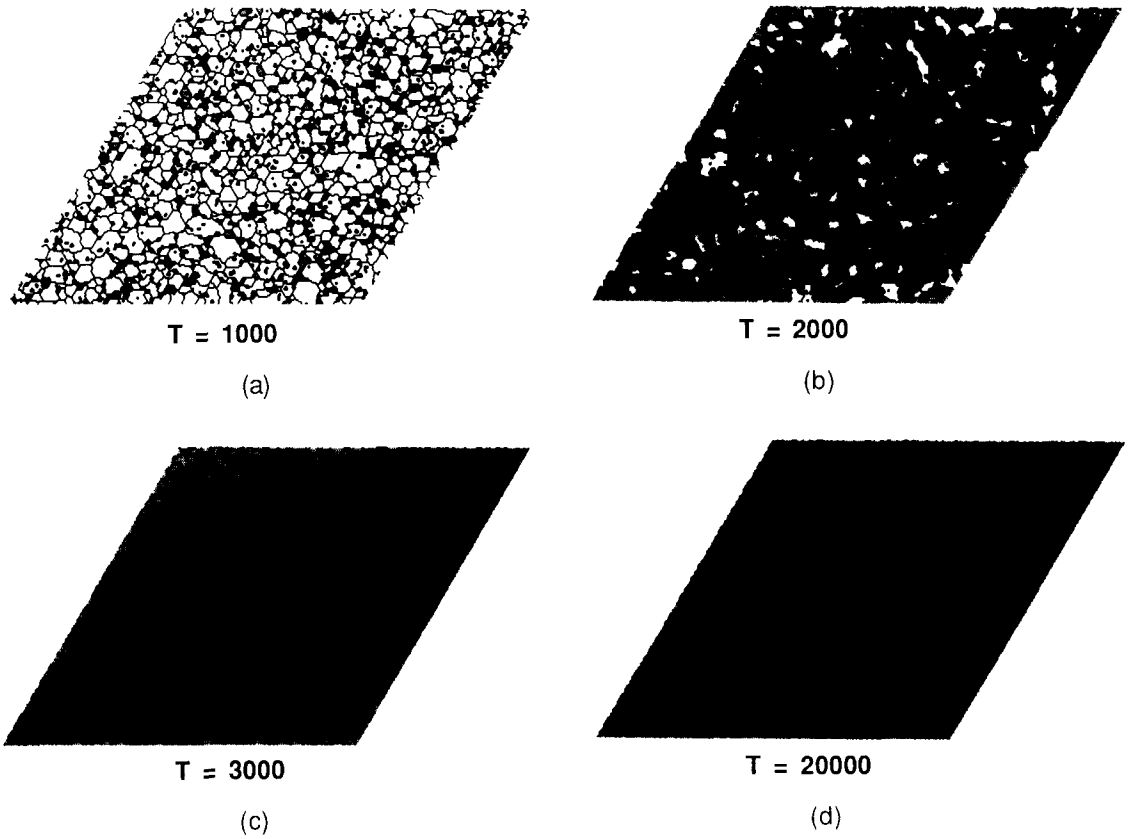

Fig. 6. Simulated microstructure generated with a nucleation rate of 5/mcs and an energy storage rate of 10^{-3} J/mcs at times (a) 1000 mcs (before the first stored energy peak), (b) 2000 mcs (after the first stored energy peak), (c) 3000 mcs (close to the maximum grain size) and (d) 20,000 mcs (the asymptotic grain size).

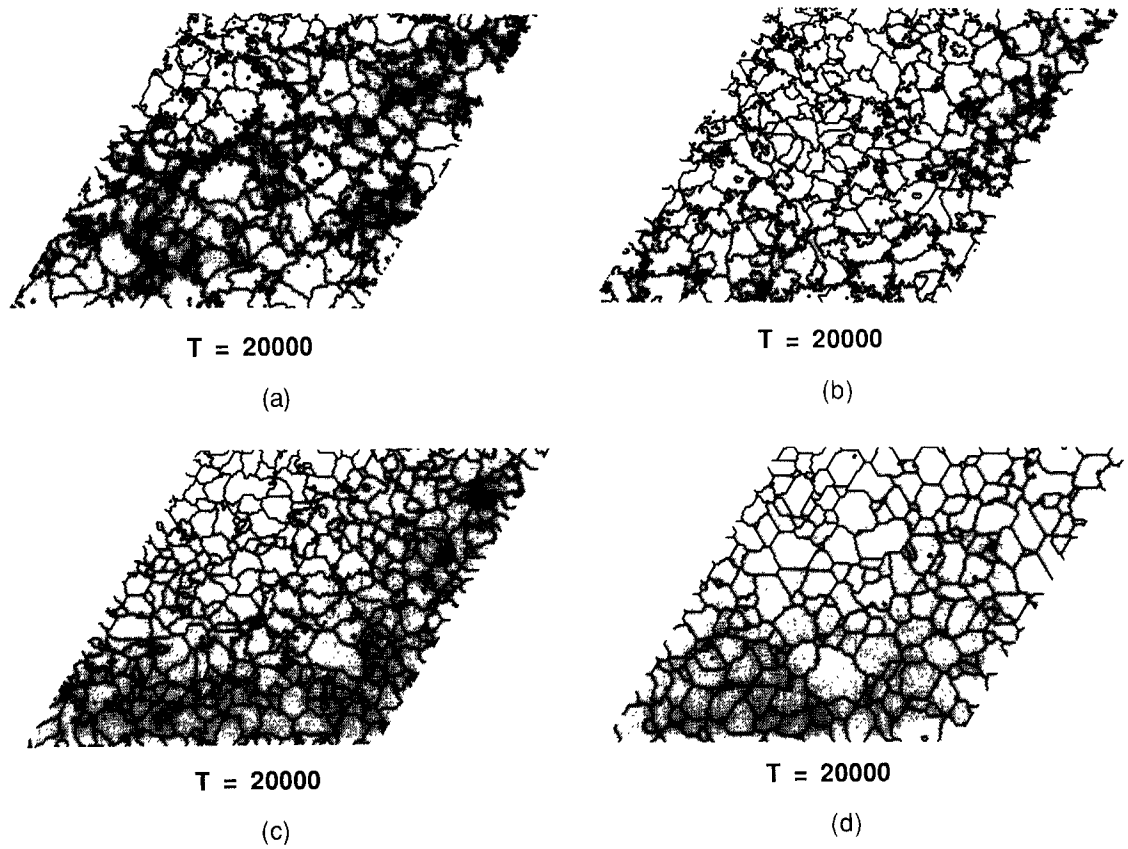

Fig. 7. Simulated microstructure for long times (20,000 mcs) for constant nucleation rate (5/mcs) and (a) 10^{-2} J/mcs, (b) $5 \cdot 10^{-3}$ J/mcs, (c) $2 \cdot 10^{-3}$ J/mcs and (d) $2 \cdot 10^{-4}$ J/mcs.

the fact that there is a spread in stored energy present in the model, once a significant volume fraction has recrystallized. To demonstrate the influence of the simulation conditions on the microstructures developed at long times, representative structures for a range of values of the energy addition rate are shown in Fig. 7. The microstructures show some similarities to one another but the highest storage rate, 10^{-2} per mcs, shows a much higher density of small grains, presumably nucleating grains, than does the lowest rate, $2 \cdot 10^{-4}$ per mcs. Also the grain boundaries show less curvature as the storage rate decreases.

The microstructures described above do not show the characteristic "necklace" structure that is often associated with dynamic recrystallization [14]. However, the short time microstructures developed during the simulation with very coarse initial grain sizes do show this type of structure, as may be seen in Fig. 8. This microstructure was formed after 2000 mcs in a simulation with an initial grain size of 12.6 at a nucleation rate of 5 per mcs and an energy addition rate of 10^{-3} J/mcs. Although nuclei are inserted into the model in a spatially random fashion, clearly only those nuclei that are in contact with the prior grain boundaries survive and grow at the low stored energies present at short times. The nucleation rate is high enough that the prior grain boundaries are completely coated with new grains. The microstructure shows clearly that "necklacing" does occur in this model albeit under relatively extreme initial conditions. Some other cases of grain refinement during dynamic recrystallization (such as in Fig. 6) do not show "necklacing". The observation that the present model does not always produce a "necklaced" microstructure in the initial stages of dynamic recrystallization may be related to the relation between the size of the potential nuclei and the grains. The smallest potential nucleus employed in the present model consists of 3 sites, while the average number of sites per grain in the starting microstructures used for the most of the simulation runs was 40. Accordingly, the grains are only four times the nucleus diameter. This is equivalent to a mean grain size of 0.4–4 μm, given that typical hot-worked subgrains are in the size range of 0.1–2 μm. This is clearly a very fine grain size and is unlikely to be found in real systems. On the other hand, "necklaced" structures were observed when the initial mean number of sites per grain size was 160, which is equivalent to real grain sizes in the range of 0.8–8 μm. Although still fine grained, such grain sizes are more representative of the sizes found in real systems.

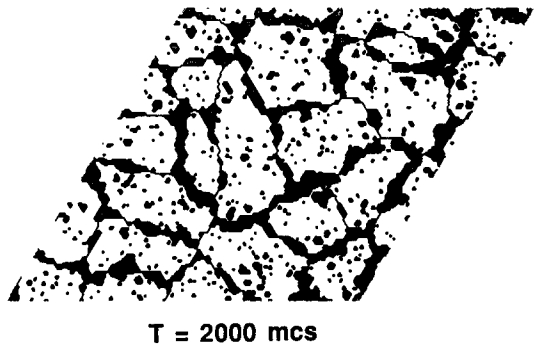

Fig. 8. Simulated microstructure generated with a nucleation rate of 5/mcs and an energy storage rate of 10^{-3} J/mcs, from an initial microstructure with a grain size of 12.6, at 2000 mcs.

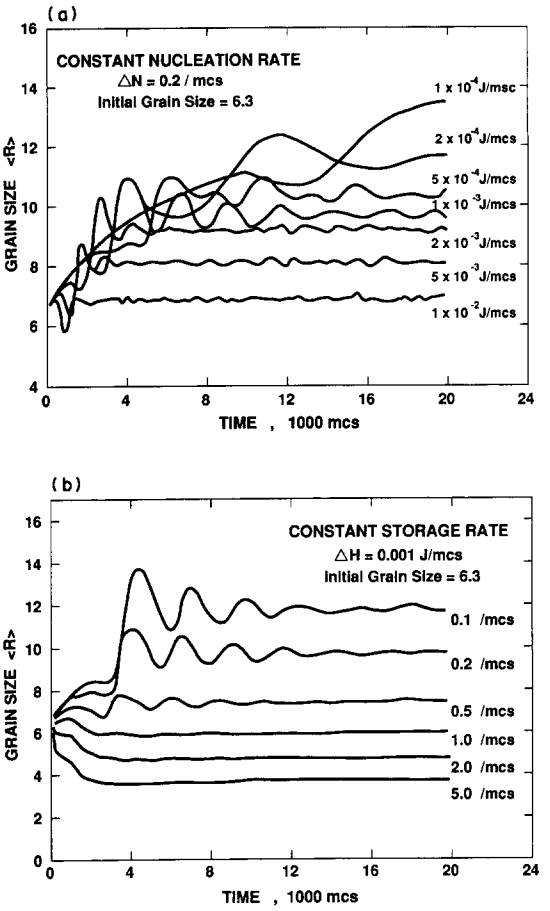

Fig. 9. Plot of mean grain size vs time (a) for different energy storage rates and a fixed nucleation rate of $\Delta N = 0.2$/mcs and (b) for different nucleation rates and a fixed energy storage rate of $\Delta H = 10^{-3}$ J/mcs.

The microstructures displayed in Figs 5–8 show that grain size varies with time during the dynamic recrystallization process and is sensitive to both the energy storage rate ΔH and the nucleation rate ΔN. This observation is quantified in Fig. 9(a) and (b), where the mean grain size, $\langle R \rangle$, is plotted as a function of time for various energy storage rates and nucleation rates, respectively. Examination of Fig. 9(a) and (b) show that there exists a short transient in the time dependence of the grain size which is followed by a period of oscillating size and, at long times, a mean grain size which is essentially time independent. In contrast to the stored energy vs time plots, shown in Fig. 2, the oscillations in the grain size are observed at low nucleation rates but not

at high ones. Also comparison of Figs 2 and 9 show that the oscillations in grain size occur with the same period as do the oscillations in the stored energy. It is interesting to note, however, that the oscillations in grain size and stored energy appear to be out of phase by approximately a quarter period. This is shown most clearly in a parametric plot of mean grain size vs mean stored energy (Fig. 10) where time is the free parameter and where $\Delta N = 0.1$/mcs and $\Delta H = 10^{-3}$ J/mcs. After an initial transient, the data describe a spiral that converges to a point as the oscillations damp out. If the mean grain size and the stored energy were in phase, the plot would be a straight line. The initial transient behavior observed in the time dependence of the grain size, before the onset of regular oscillations, does not occur in the stored energy vs time plots. Although the transients observed are indeed distinct from the later oscillatory behavior, hints of such oscillation may also be observed within the transient regime. Additionally, the temporal extent of the transient regime is nearly equal to the grain size oscillation period observed at slightly later times.

The asymptotic or steady state grain size varies with both the energy storage rate and nucleation rate. Figure 11(a) and (b) show the dependence of the asymptotic grain size on the energy storage rate and nucleation rate, respectively. The asymptotic grain size decreases with increasing energy storage rate and with increasing nucleation rate. This is to be distinguished from the stored energy data (Fig. 4), where the stored energy increases storage rate but decreases with increasing nucleation rate. A numerical fit to the data in Fig. 11 shows that the asymptotic grain size decreases as $\Delta H^{-\alpha}$, where $\alpha = 0.13$ and $\Delta N^{-\beta}$, where $\beta = 0.30$.

4. DISCUSSION

It is evident from the results described above that the simulation experiments initially produce the temporal oscillations in both stored energy and grain size that are associated with dynamic recrystallization. The stored energy data, however, are not presented in a manner which provides a ready comparison with typical flow curves such as those shown in Fig. 1. Nevertheless, the stored energy can be directly converted to a pseudo-flow stress by recognizing that the stored energy is directly proportional to the dislocation density, which is, in turn, proportional to the square of the flow stress [equation (2)]. Then, if it is assumed that the work hardening rate is independent of the strain rate ($\epsilon = \Delta H t$), the stored energy vs time curves [Fig. 2(a)] may be recast as constant strain rate, stress–strain curves (see Fig. 12). These curves show many of the characteristics of the flow curves obtained from physical experiments; namely, the flow stress exhibits an initial peak which is followed by flow stress oscillations that decay as the strain is increased until an essentially constant value of the flow stress is established. The initial peak in the simulated flow curve corresponding to an energy storage rate of 0.1 J/mcs is not seen in Fig. 12 since it occurs at strains beyond those shown in the figure. Also, at the lower strain rates, the amplitude of the

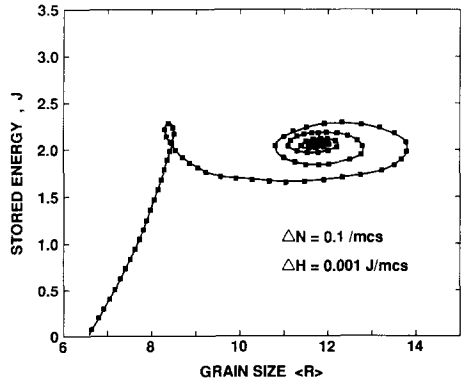

Fig. 10. Plot of stored energy vs grain size from a simulation with an energy storage rate of $\Delta H = 10^{-3}$ J/mcs and a nucleation rate of $\Delta N = 0.2$/mcs.

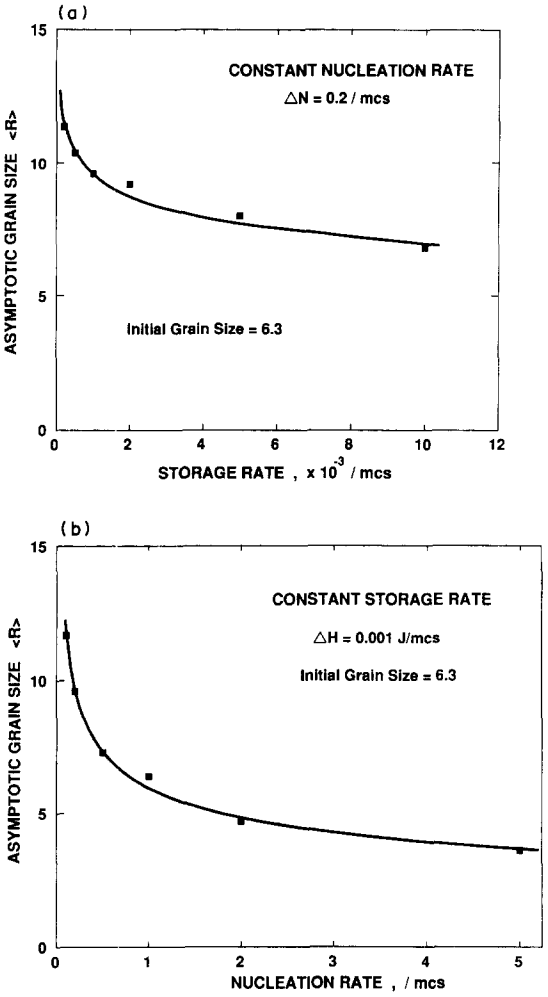

Fig. 11. Plot of asymptotic grain size vs (a) energy storage rate for a fixed nucleation rate of $\Delta N = 0.2$/mcs and (b) nucleation rate for a fixed energy storage rate of $\Delta H = 10^{-3}$ J/mcs.

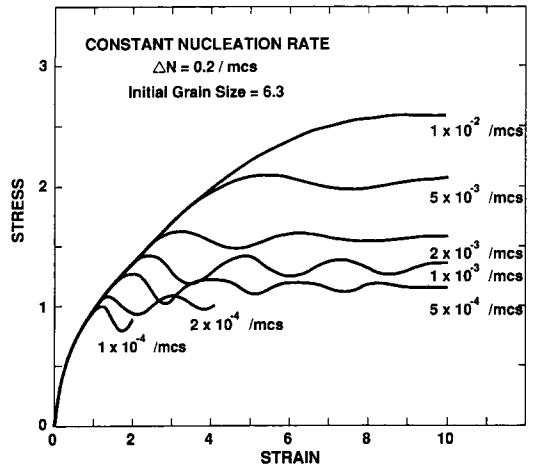

Fig. 12. The data of Fig. 2(a) replotted as a series of pseudo stress–strain curves by application of $\sigma = \sqrt{H}$ and the assumption that the work-hardening rate is directly proportional to strain rate.

oscillations in flow stress does not attenuate as quickly as the curves obtained in physical experiments. Furthermore, the simulations do not incorporate the rate sensitivity of the yield stress and initial hardening rate that is apparent in the experimental data.

It is of interest to note that the curves in Fig. 3 imply that the peak and steady state flow stress exhibit a power-law dependence on strain rate. The measured strain rate sensitivity of these two stresses were found to be 0.33 and 0.37, respectively. In physical experiments on dynamic recrystallization the strain rate sensitivity of the flow stress is typically the same as that observed in materials that soften during deformation by dynamic recovery alone, i.e. in the 0.15–0.25 range. Thus the present simulations, where no rate dependence of work hardening is included, produces a rate sensitivity of the flow stress that is ~ 1.7 times that observed in physical experiments. Here the rate sensitivity arises from the rate dependence of the softening due to recrystallization that naturally evolves from the model. It should be noted, however, that in the simulations used to produce Fig. 12, the nucleation rate was held constant. In the simulations performed at constant ΔH and ΔN it was shown that when the nucleation rate is increased the stored energy, and therefore the flow stress, is decreased. Accordingly, if the nucleation rate was coupled to the rate of energy storage so that higher rates of nucleation occurred at the higher energy storage rates, the rate sensitivity of the flow stress would more closely approach that observed in physical experiments. The fact that the simulated flow stress exhibits a strain rate sensitivity that closely approaches that observed in physical experiments points to a persistent complication in the interpretation of flow stress in materials that undergo dynamic recrystallization; namely, the relative importance and interaction between the two softening mechanisms, dynamic recovery and dynamic recrystallization.

It is clear from Fig. 12 that the strain at the peak flow stress, ϵ_p, increases with increasing strain rate. The values of ϵ_p obtained from the simulations with constant ΔN and varying ΔH are plotted logarithmically as a function of strain rate in Fig. 13(a). This figure may be compared with data obtained on copper [26] that is similarly plotted in Fig. 13(b). The simulation results show the same trend as that observed in the physical experiments but the slope of the curve is greater than the value of 0.15 obtained for copper and several steels [27]. Examination of Fig. 2(b) shows that the time to reach the maximum in stored energy decreases as the nucleation rate increases so that if the nucleation rate increases with strain rate, the slope of the curve in Fig. 13(a) would be reduced and more closely approach that of Fig. 13(b). This comparison again suggests that a coupling of the nucleation rate and energy storage rate would bring the simulation into closer agreement with the experimental results.

In discussions of dynamic recrystallization, it is generally assumed that there is a critical strain, ϵ_c, for

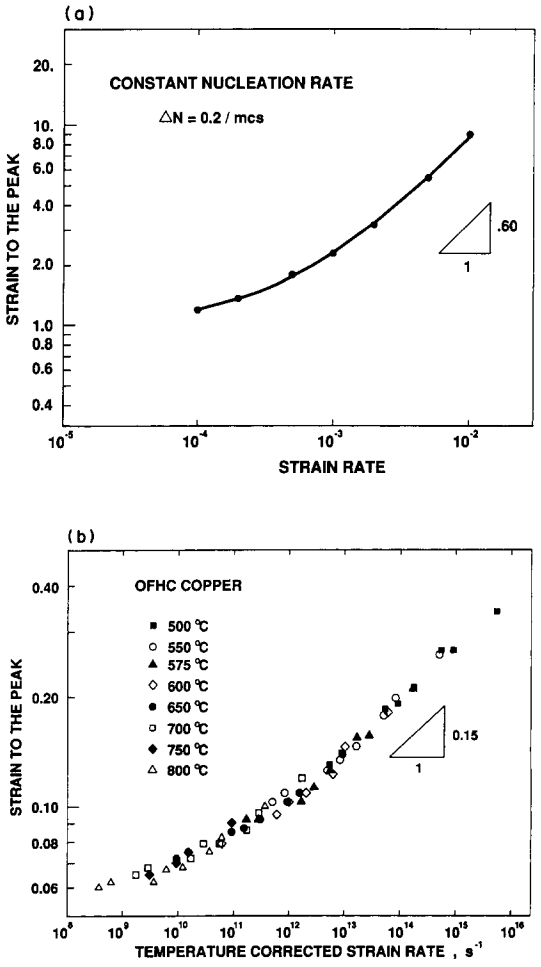

Fig. 13. Plot of the pseudo strain to the flow stress peak (a) vs pseudo strain rate for simulations with a fixed nucleation rate of $\Delta N = 0.2$/mcs and various ΔH; (b) vs a temperature corrected strain rate for experiments on copper.

the onset of the recrystallization process. From careful metallographic studies of hot worked steel, Rossard [8] concluded that ϵ_c is about equal to $0.8\,\epsilon_p$. Inasmuch as the detection of newly recrystallized grains in a deformed matrix is difficult, it can be assumed that this assessment of the value of ϵ_c is based upon the presence of a small volume fraction of new grains, say about 5%. Examination of the microstructures generated by the simulations used to produce Fig. 12 show that $\epsilon_{5\%}$ is in the range of 0.67 to $0.86\,\epsilon_p$. This observation is made clearer in Fig. 14 in which the stored energy and the fraction recrystallized, F, are plotted as a function of time; F is calculated as one minus the fraction of material that has never recrystallized and so it has the value of one after the first cycle of recrystrallization is complete. In this respect, the simulations generate microstructural changes that correlate with the flow stress variations in much the same way as is observed in physical experiments.

As mentioned above, oscillations in the stored energy, and therefore, the flow stress, occur for all energy storage and nucleation rates. Such oscillations are most pronounced at lower energy storage and nucleation rates. Both of these conditions lead to large grain sizes. This is consistent with the observations of Sakai and co-workers [12–16], who associated oscillations in the flow curves with a coarsening of grain size. Nevertheless, the simulations clearly show that the occurrence of such oscillations is independent of whether the asymptotic grain size is larger or smaller than the initial grain size. On the other hand, the rate at which the oscillations decay seems to be correlated with asymptotic grain size; that is, a slow decay for large grain sizes and fast decay for small grain sizes. In other words, the stored energy oscillations are underdamped at large asymptotic grain sizes but become more severely damped, or overdamped, in the limit of small grain sizes. Comparisons of Figs 2 and 5 show that the degree of damping is not simply determined by the asymptotic grain size. The simulations with the largest energy storage rates and smaller nucleation rates, for example $\Delta H = 0.01$ J/mcs and $\Delta N = 0.2$/mcs, are significantly more strongly damped than in those simulations with higher nucleation and lower energy storage rates, for example $\Delta H = 0.001$ J/mcs and $\Delta N = 5.0$/mcs, although the latter situation results in a much finer, final grain size.

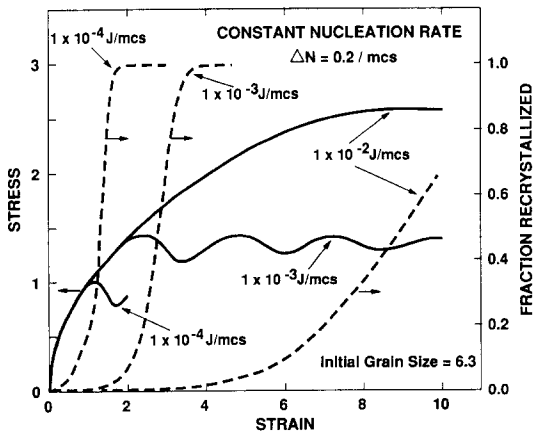

Fig. 14. Plot of stress vs strain and fraction recrystallized vs strain (for the first cycle of recrystallization) for three different storage rates, $\Delta H = 10^{-4}$, 10^{-3} and 10^{-2} J/mcs. The solid lines denote stress and the dashed lines denote fraction recrystallized. Note that the fraction recrystallized at the first peak in stress lies in the range 0.1–0.4.

The association of oscillations with dynamic recrystallization extends beyond the flow curves. Pronounced oscillations in the stored energy vs time plots are always accompanied by oscillations in the mean grain size vs time plots, as shown in Fig. 9. The similarity between the periods of the oscillation in the stored energy and grain size show that the grain size is closely coupled to the stored energy. Clearly, the onset and/or completion of a recrystallization cycle affects both the grain size and the stored energy. However, the interdependence of grain size and stored energy is not as strong as is suggested by this correlation. In order to investigate the correlation between grain size and stored energy, three additional sets of simulations were performed with identical dynamic recrystallization parameters, ΔH and ΔN, but with three different initial grain sizes. Figure 15(a) and (b) show the time evolution of the stored energy and grain size, respectively. While the stored energy vs time plots are completely insensitive to the initial grain size, the grain size vs time plots show considerable differences over the first recrystallization cycle. However, following the first stored energy oscillation or recrystallization cycle, the grain size evolution history is completely independent of the initial grain size. Consequently, the asymptotic grain sizes and stored energies are completely determined by the choice of the dynamic recrystallization parameters, ΔH and ΔN.

All of these results suggest that the microstructural evolution occurring during dynamic recrystallization has three distinct stages: an initial microstructure dependent transient stage, I, an initial microstructure independent stage, II, and a steady state stage, III. Stage I corresponds to the first recrystallization cycle and is characterized by a rapid, irregular change in grain size over a time period corresponding to the oscillation period. Stage II shows oscillations in both the stored energy and grain size. Finally, in Stage III, the grain size and stored energy are time independent. The division betwen Stages II and III is somewhat arbitrary however, since the oscillations are damped out in a continuous manner. The division between Stages I and II, on the other hand, is quite abrupt whereas in Stages II and III the microstructure is completely specified by the dynamic recrystallization parameters, ΔH and ΔN. A single composite parameter has not been identified which describes both of the main microstructural features; namely, the asymptotic grain size and the asymptotic stored

energy. The asymptotic stress (square root of the stored energy) is plotted as a function of the asymptotic grain size in Fig. 16 for the entire range of ΔH and ΔN simulated (solid lines with points). This figure shows that very different behavior is obtained when the nucleation rate is varied at fixed storage rate when the storage rate is varied at fixed nucleation rate. Specifically, as the storage rate is increased the ratio of grain size to stress decreases while the converse applies to variations in the nucleation rate. Varying the energy storage rate affects the asymptotic stress more than the asymptotic grain size. By contrast, varying the nucleation rate affects the asymptotic grain size more than the asymptotic stress. Clearly, it is possible to create different dynamically recrystallized samples with the same asymptotic grain size but with completely different stored energies, and vice versa, depending on the nucleation rate and energy storage rate. The asymptotic grain sizes and stresses achieved in Stage III are not static features but represent a dynamic equilibrium in a microstructure

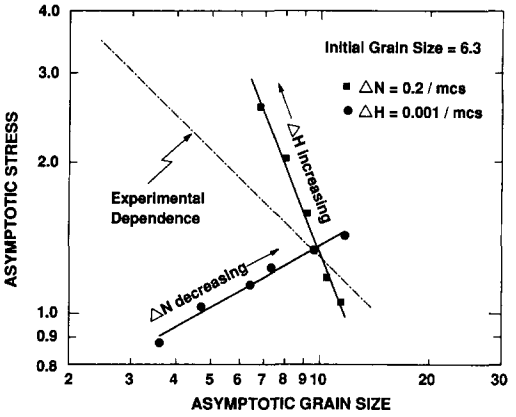

Fig. 16. A logarithmic plot of asymptotic stress as a function of asymptotic grain size (solid lines with points) for the entire range of nucleation and energy storage rates examined. The broken curve represents the experimentally observed relationship.

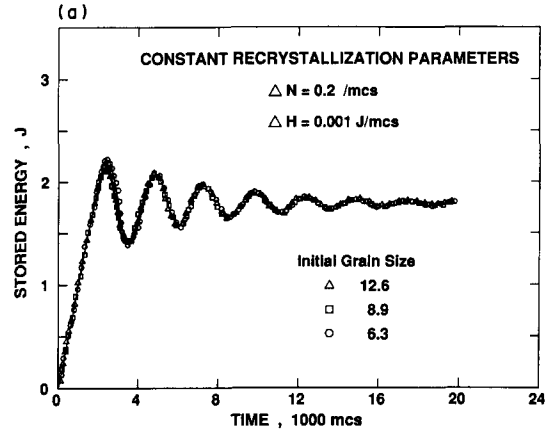

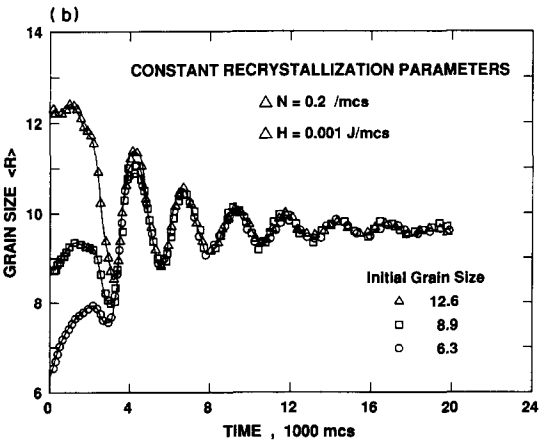

Fig. 15. (a) Plot of the time evolution of stored energy for a fixed nucleation rate of $\Delta N = 0.2$/mcs and a fixed energy storage rate of $\Delta H = 10^{-3}$ J/mcs, for initial grain sizes of 6.3, 8.9 and 12.6. (b) Plot of the time evolution of grain size for a fixed nucleation rate of $\Delta N = 0.2$/mcs and a fixed energy storage rate of $\Delta H = 10^{-3}$ J/mcs, for initial grain sizes of 6.3, 8.9 and 12.6.

which is very much in flux. For comparison with experiment, Fig. 16 also has plotted (dotted line) the experimental trend for asymptotic stress vs grain size [7, 25]. Clearly, the simulations, under the constant nucleation rate condition, produce a stronger dependence than is observed in practice (i.e. —1.8 power vs −0.7) [28]. Nevertheless, the simulation results suggest that a very good fit to the experimental relationship between stress and grain size could be obtained for a particular choice of the functional dependence of nucleation rate on storage rate, namely, a weak positive dependence of nucleation rate on storage rate. It should be noted that this same conclusion was drawn from the observed strain rate dependence of the asymptotic flow stress, of the maximum stress and of the strain to the maximum stress.

5. CONCLUSIONS

A Monte Carlo model for grain growth and recrystallization has been developed in which the stored energy of the grains is increased at a fixed rate and embryonic new grains are continually added at a constant rate. The basic result is that temporal oscillations are observed both in the grain size and in the stored energy which is analogous to the flow stress. These oscillations are observed over almost the entire range of recrystallization parameters examined (energy storage rate, nucleation rate, initial grain size) and damp out over time periods that decrease with increasing storage rate and increasing nucleation rate. The oscillations in both grain size and stored energy have the same period but are out of phase by approximately one quarter of a period. Examination of the simulated dynamic recrystallization microstructures which were formed under the same conditions but with different initial grain sizes shows that the evolution of the microstructure may be divided into three distinct stages: an initial

microstructure *dependent* transient stage, an initial microstructure *independent* transient stage, and a steady state stage. While necklacing was observed in these simulations under some circumstances, it is apparent that it is not a necessary condition for grain refinement in dynamic recrystallization. This phenomenon is associated with refinement of the relatively coarse initial microstructure and overdamped oscillations in the flow stress. Therefore, even when there are no obvious oscillations in the flow curve and no necklacing is observed, dynamic recrystallization cannot be precluded.

Finally, we note that while the simulation provides a complete description of the microstructure and an analog of the flow curve as a function of the parameters defining a dynamic recrystallization experiment (ΔN, ΔH and initial grain size), these simulations require the addition of no empirical parameters (e.g. critical strains for the beginning and end of recrystallization) which are integral parts of the extant theoretical models of dynamical recrystallization. These results further suggest that a weak positive dependence of nucleation rate (ΔN) on storage rate (ΔH) in our model would produce a reasonable fit with several experimentally observed trends.

REFERENCES

1. J. N. Greenwood and H. K. Worner, *J. Inst. Metals* **64,** 135 (1939).
2. R. C. Gifkins, *J. Inst. Metals* **81,** 417 (1952–1953).
3. R. C. Gifkins, *J. Inst. Metals* **87,** 255 (1958–1959).
4. S. Steinemann, *Beitrage Geol. Schweiz (Hydrol.)* **10,** 1 (1958).
5. C. M. Sellars and W. J. McG. Tegart, *Mém. scient. Revue Metall.* **63,** 731 (1959).
6. C. Rossard and P. Blain, *Mém. scient. Revue Metall.* **56,** 285 (1966).
7. M. J. Luton and C. M. Sellars, *Acta metall.* **17,** 1033 (1969).
8. C. Rossard, in *Proc. 3rd Int. Conf. on the Strength of Metals and Alloys*, Inst. of Metals and Iron and Steel Inst., London (1973).
9. J. P. Sah, G. J. Richardson and C. M. Sellars, *Metal Sci.* **8,** 325 (1974).
10. H. P. Stüwe and B. Ortner, *Metal Sci.* **8,** 161 (1974).
11. R. Sandström and R. Lagneborg, *Acta metall.* **23,** 387 (1975).
12. S. Sakui and T. Sakai, *Tetsu-to-Hagane* **62,** 856 (1976).
13. S. Sakui and T. Sakai, *Tetsu-to-Hagane* **63,** 856 (1977).
14. J. J. Jonas and T. Sakai, in *Proc. 24ème Colloque de Métallurgie, Les Traitments Thermomécaniques*, p. 35. ISTN, Saclay (1981).
15. T. Sakai and J. J. Jonas, *Acta metall.* **32,** 189 (1984).
16. L. Blaz, T. Sakai and J. J. Jonas, *Metals Sci.* **17,** 609 (1983).
17. L. Blaz and A. Korbel, *Metals Sci. Tech.* **5,** 1186 (1989).
18. M. Ueki, M. Hattori, S. Horie and T. Nakamura, *Trans. Iron Steel Inst. Japan* **26,** 907 (1987).
19. J. L. Nazabal, J. J. Urcola and M. Fuentes, *Mater. Sci. Engng* **86,** 93 (1987).
20. M. P. Anderson, D. J. Srolovitz, P. S. Sahni and G. S. Grest, *Acta metall.* **32,** 783 (1984).
21. D. J. Srolovitz, M. P. Anderson, P. S. Sahni and G. S. Grest, *Acta metall.* **32,** 793 (1984).
22. D. J. Srolovitz, G. S. Grest and M. P. Anderson, *Acta metall.* **32,** 793 (1988).
23. D. J. Srolovitz, G. S. Grest, M. P. Anderson and A. D. Rollett, *Acta metall.* **36,** 2115 (1988).
24. P. S. Sahni, D. J. Srolovitz, G. S. Grest, M. P. Anderson and S. A. Safran, *Phys. Rev.* **B28,** 2705 (1983).
25. J. J. Jonas, C. M. Sellars and W. J. McG. Tegart, *Metal Rev.* **14,** 1 (1969).
26. K. C. Cadien, M. J. Luton, unpublished research.
27. C. M. Sellars, in *Hot Working and Forming Processes* (edited by C. M. Sellars and G. J. Davis), p. 3. Metals Soc., London (1980).
28. B. Derby, *Acta metall.* **39,** 955 (1991).